Electronic Supplementary Material (ESI) for Journal of Materials Chemistry A.

Supporting information for

Triggering High Conductive $FePSe_3$ with Cu-based Coordination towards All-climate Ultrafast Sodium Ions Storage

Figures and Captions

Fig.S1 TG curves of the as-resulted samples about FP (a), FPS-1 (b) and FPS-2 (c)

Fig.S2 The analysis of elements valence: Full XPS spectra of FP (a) and FPS-1 (d), Fe2p HR-XPS of FP (b) and FPS-1 (e), P2p HR-XPS of FP (c)

Fig.S3 SEM, EDS, Mapping images of FP (A1-A3), FPS-1 (B1-B6), FPS-2 (C1, C2)

Fig.S4 TEM images of FP (A1, A2), FPS-1 (B1, B2), FPS-2 (C1, C2)

Fig.S5 The cycling stability of FPS-2 and CA-FPS-2 at 10.0 A g^{-1} (a) and 20.0 A g^{-1} (b)

Fig.S6 The long-term cycling stability of CA-FPS-2 at 10.0 A g^{-1} and LT -30^{o}C

Fig.S7 The long-term CV curves at 2.0 mV s^{-1} from 1st to 30th

Fig.S8 The linear relation between log (i) and log (v)

Fig.S9 Nyquist Plots at various cycles and the relative linear of $w^{-1/2}$ with Z'' for FP (A1, A2), FPS-1 (B1, B2), FPS-2 (C1, C2)

Fig.S10 Nyquist Plots at various cycles and the relative linear of $w^{-1/2}$ with Z'' for, CA-FPS-2 (A1, A2) at RT, CA-FPS-2 (B1, B2) at LT

Fig.S11 The models of coordination with different contents before optimization and after optimization about Cu/DEGDME 1/1 (A1, A2), 1/2 (B1, B2), 1/3 (C1, C2) and 1/4 (D1, D2)

Fig.S12 SEM images of active materials, and relative Cu foils after 2000 cycles for FP (A1-A2), FPS-1 (B1-B2)

Fig.S13 Mapping images of FPS-2 after 2000 cycles

Fig.S14 Used Celgard as separations, the cycling stability of FPS-2 at 5.0 A g^{-1}

Fig.S15 SEM and Mapping images of separation (glass fiber) after 2000 cycles about FP (a), FPS-1 (b), the optical images in the inset of separations

Fig.S16 Used Celgard as separations after 300 cycles: SEM images of Cu-foils (A1), active materials (A2), separations-Celgard (B1, B2), the corresponding optical images in the inset of separations

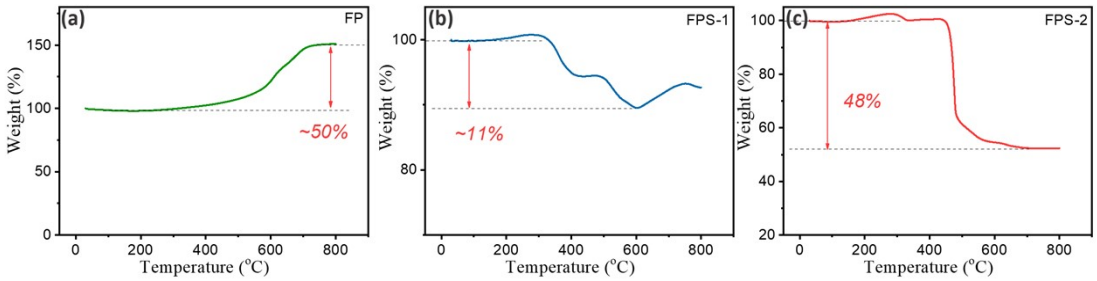

Fig.S1 TG curves of the as-resulted samples about FP (a), FPS-1 (b) and FPS-2 (c)

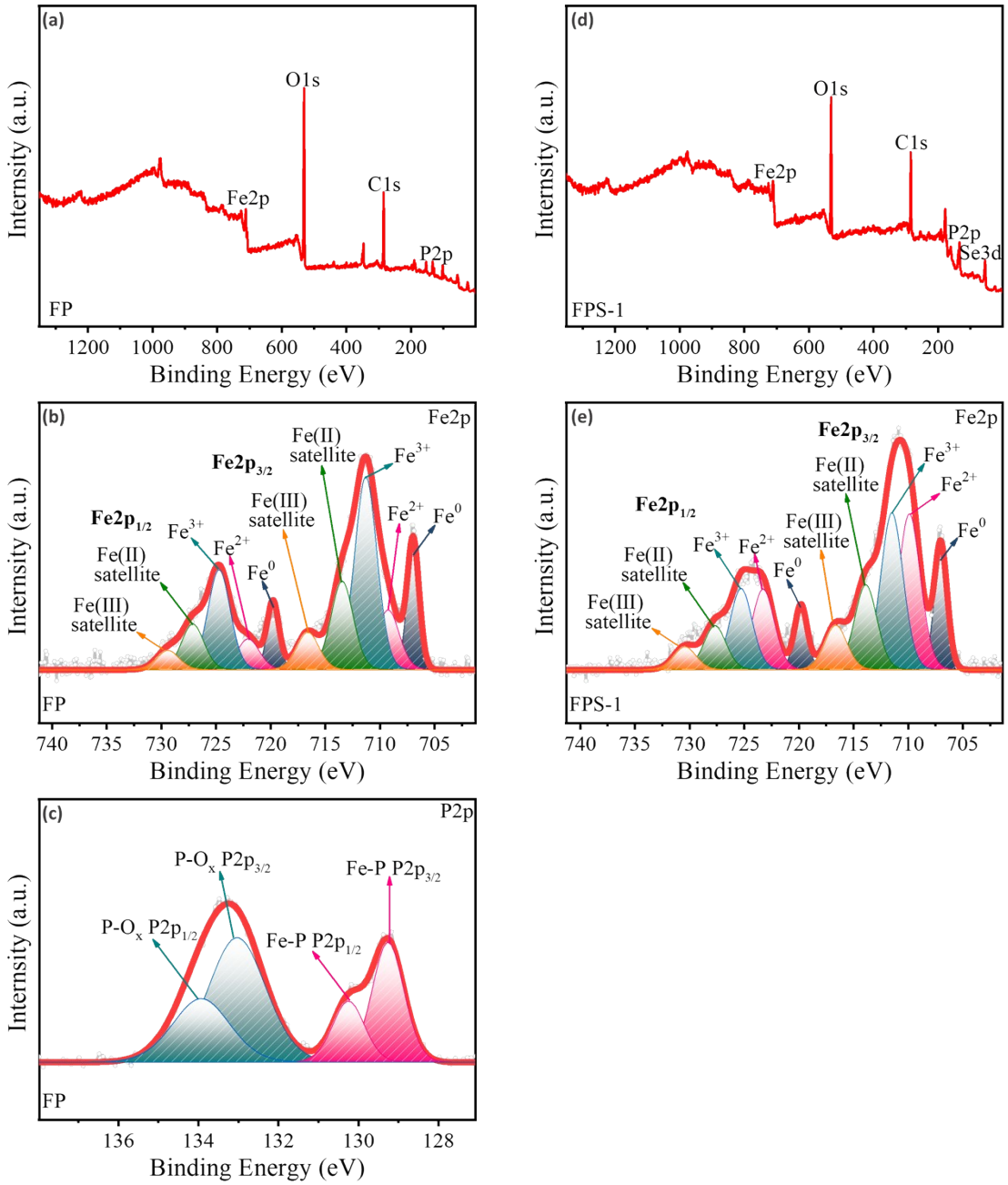

Fig.S2 The analysis of elements valence: Full XPS spectra of FP (a) and FPS-1 (d), Fe2p HR-XPS of FP (b) and FPS-1 (e), P2p HR-XPS of FP (c)

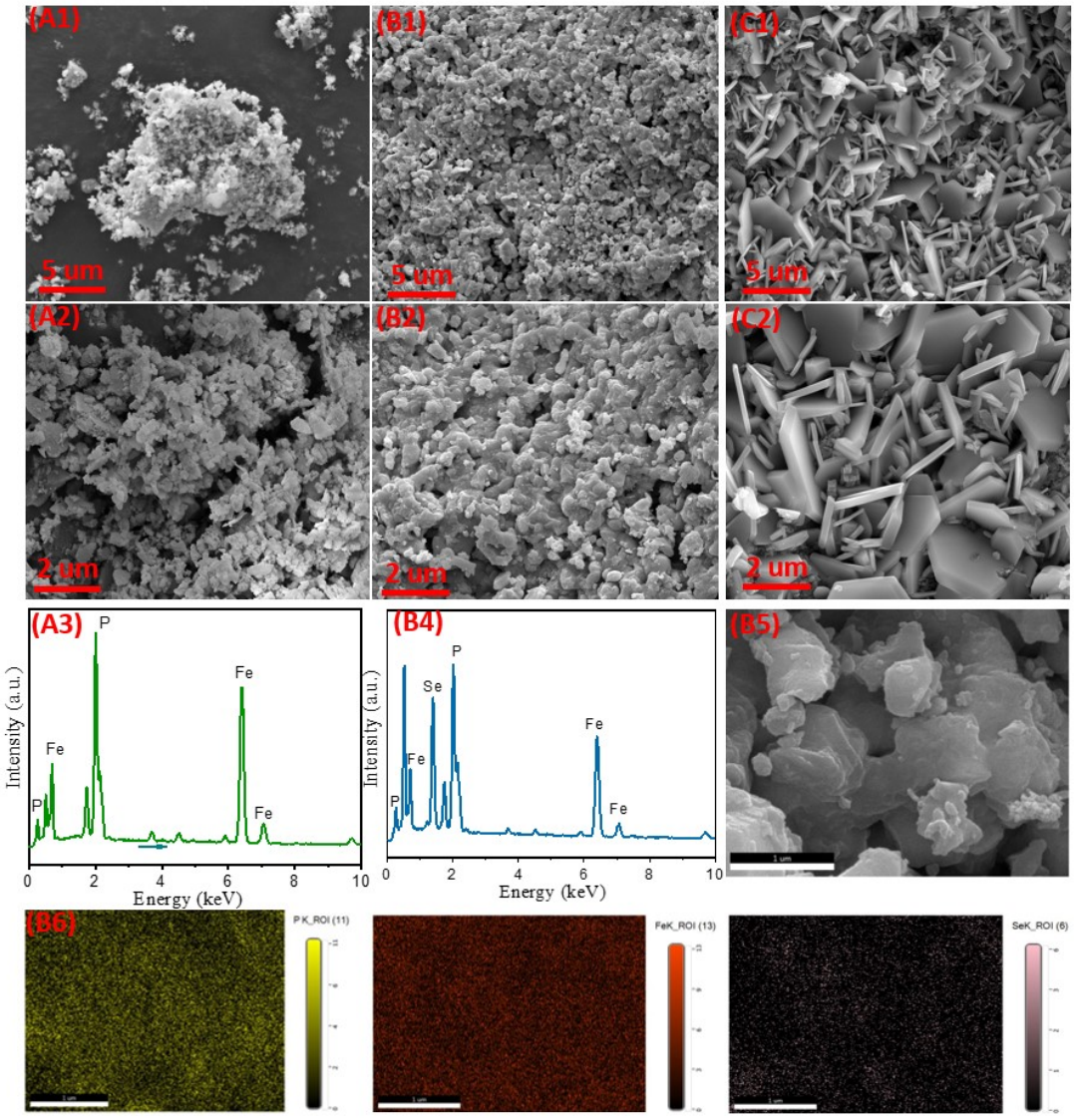

Fig.S3 SEM, EDS, Mapping images of FP (A1-A3), FPS-1 (B1-B6), FPS-2 (C1, C2)

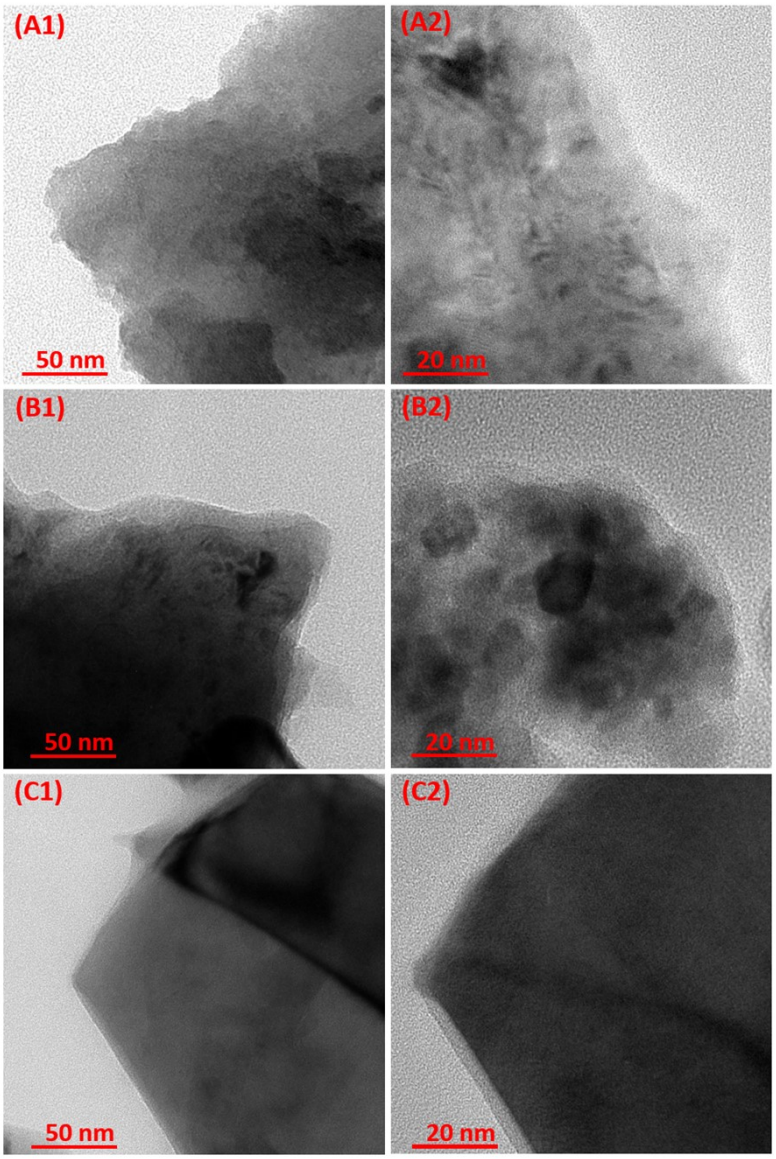

Fig.S4 TEM images of FP (A1, A2), FPS-1 (B1, B2), FPS-2 (C1, C2)

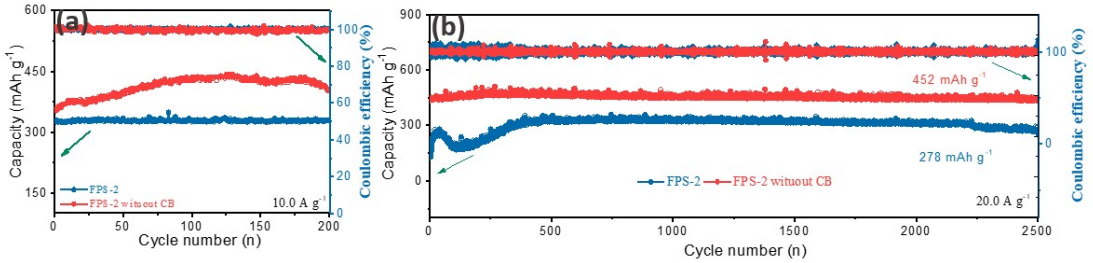

Fig.S5 The cycling stability of FPS-2 and CA-FPS-2 at 10.0 A g^{-1} (a) and 20.0 A g^{-1} (b)

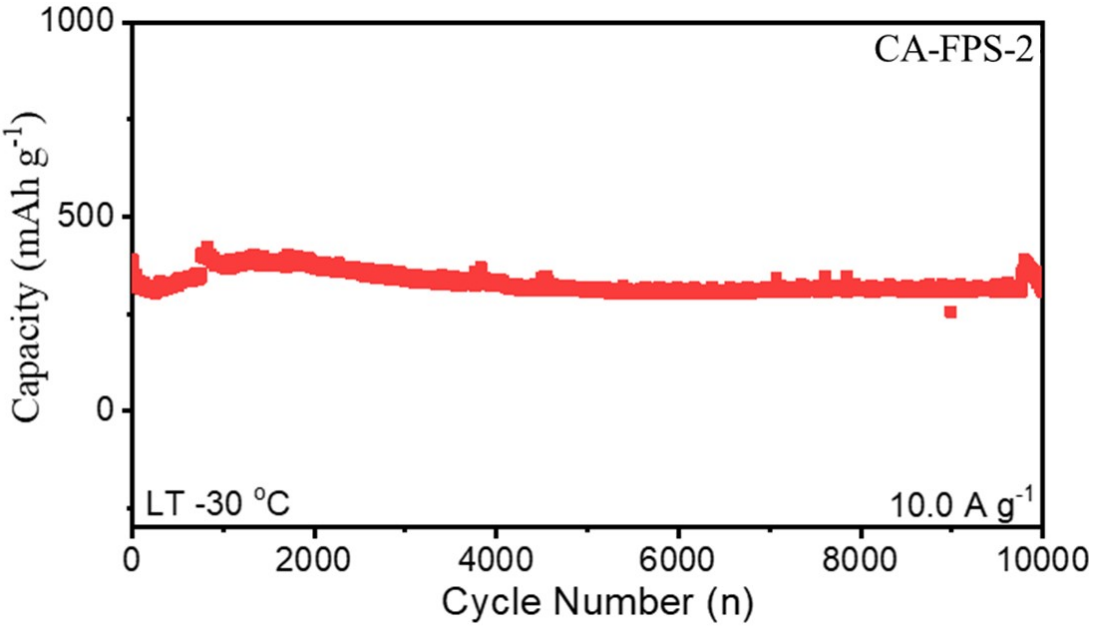

Fig.S6 The long-term cycling stability of CA-FPS-2 at 10.0 A g^{-1} and LT -30°C

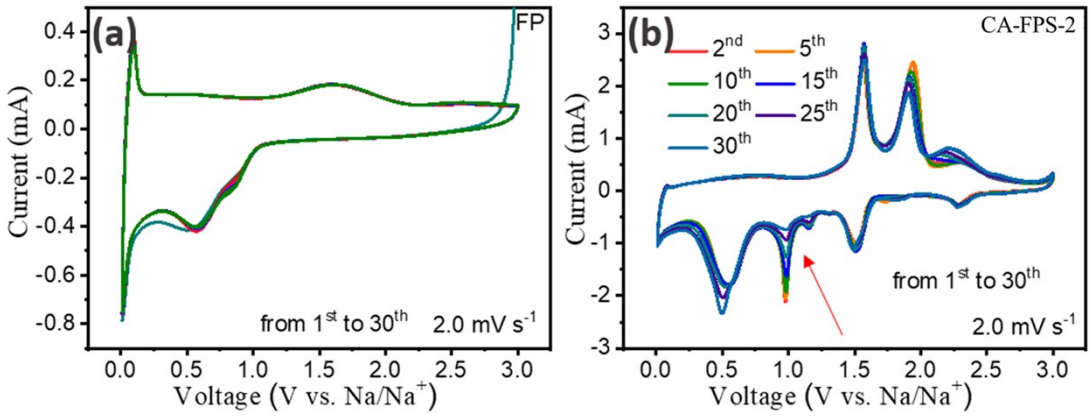

Fig.S7 The long-term CV curves at 2.0 mV s^{-1} from 1st to 30th

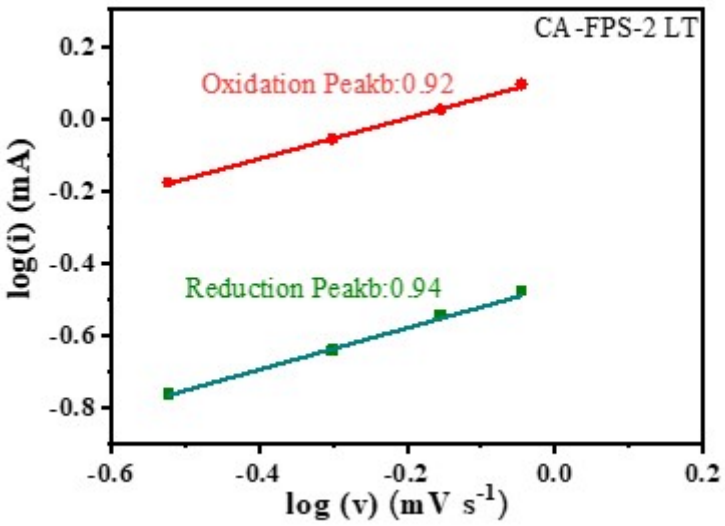

Fig.S8 The linear relation between log (i) and log (v)

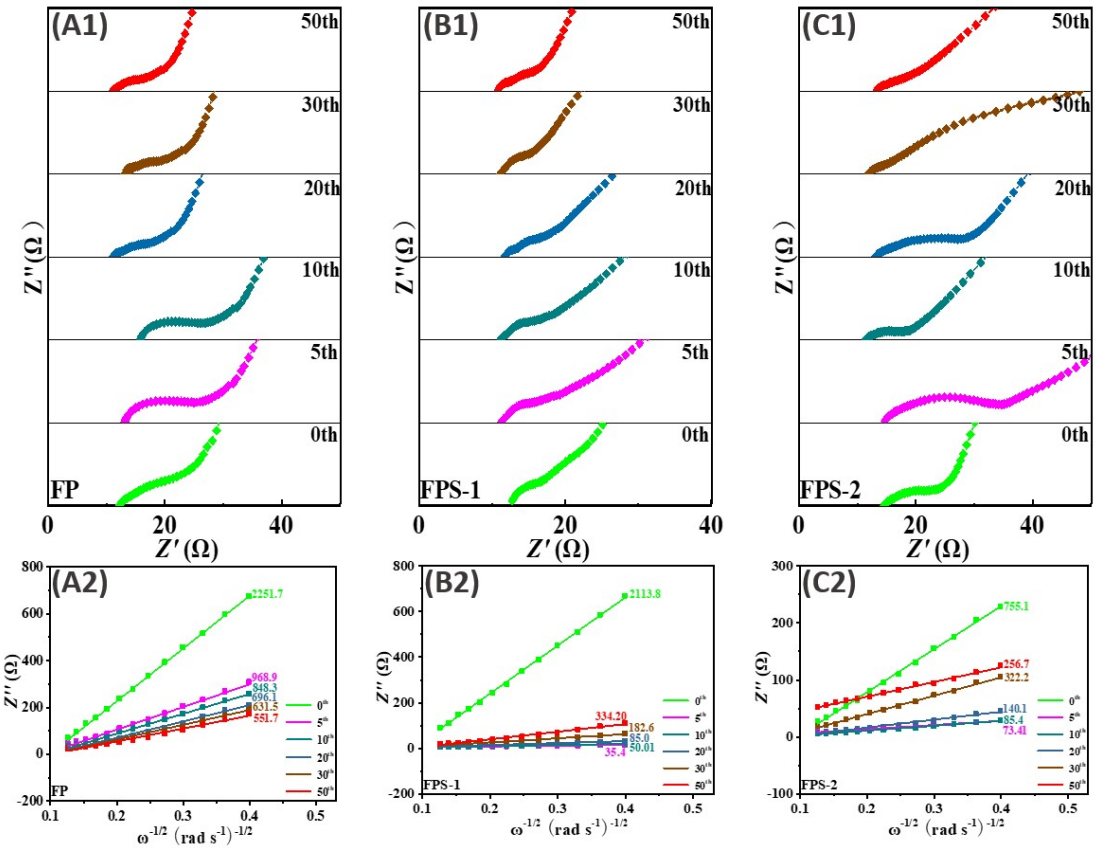

Fig.S9 Nyquist Plots at various cycles and the relative linear of $w^{-1/2}$ with Z'' for FP (A1, A2), FPS-1 (B1, B2), FPS-2 (C1, C2)

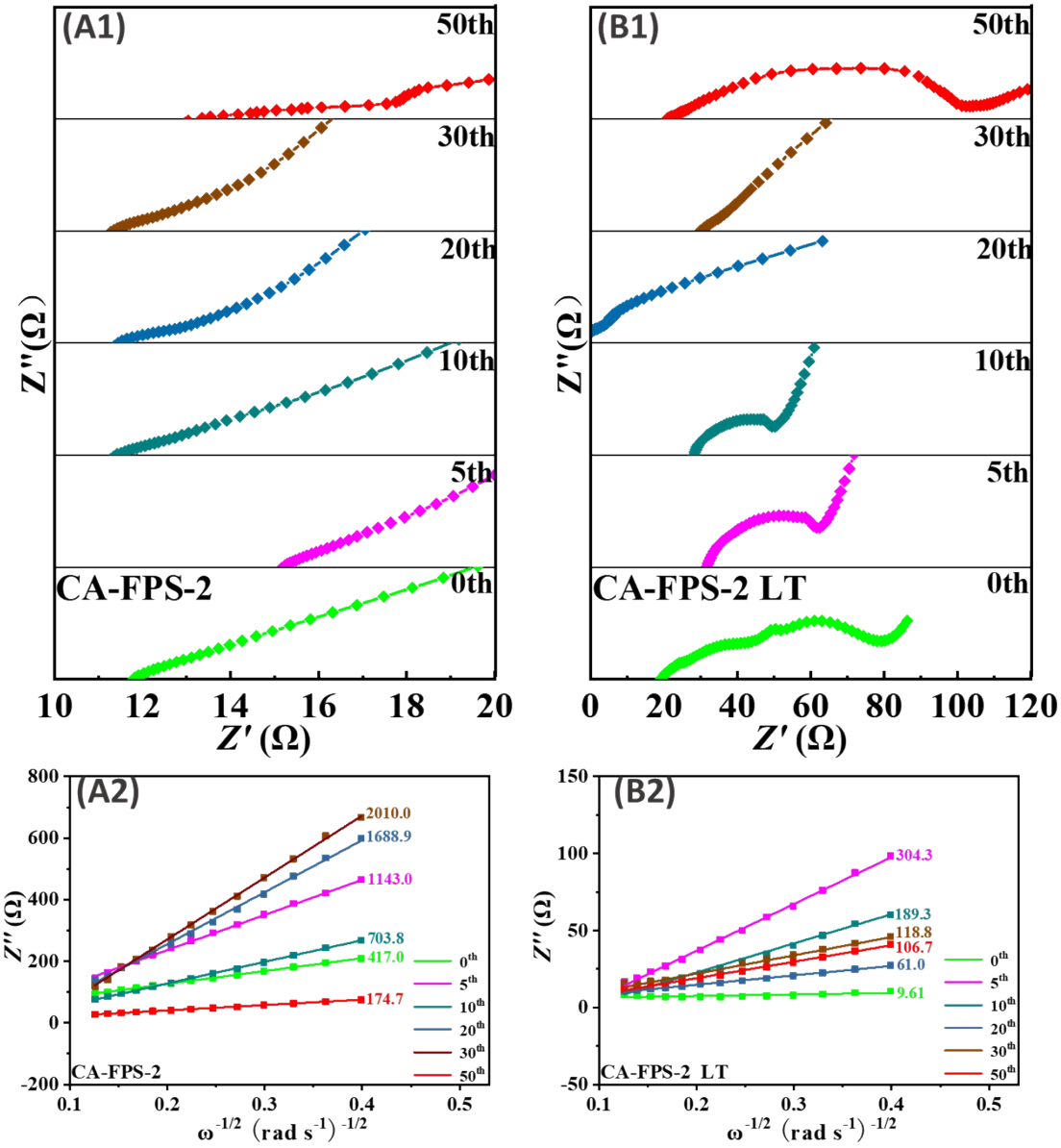

Fig.S10 Nyquist Plots at various cycles and the relative linear of $w^{-1/2}$ with Z'' for, CA-FPS-2 (A1, A2) at RT, CA-FPS-2 (B1, B2) at LT

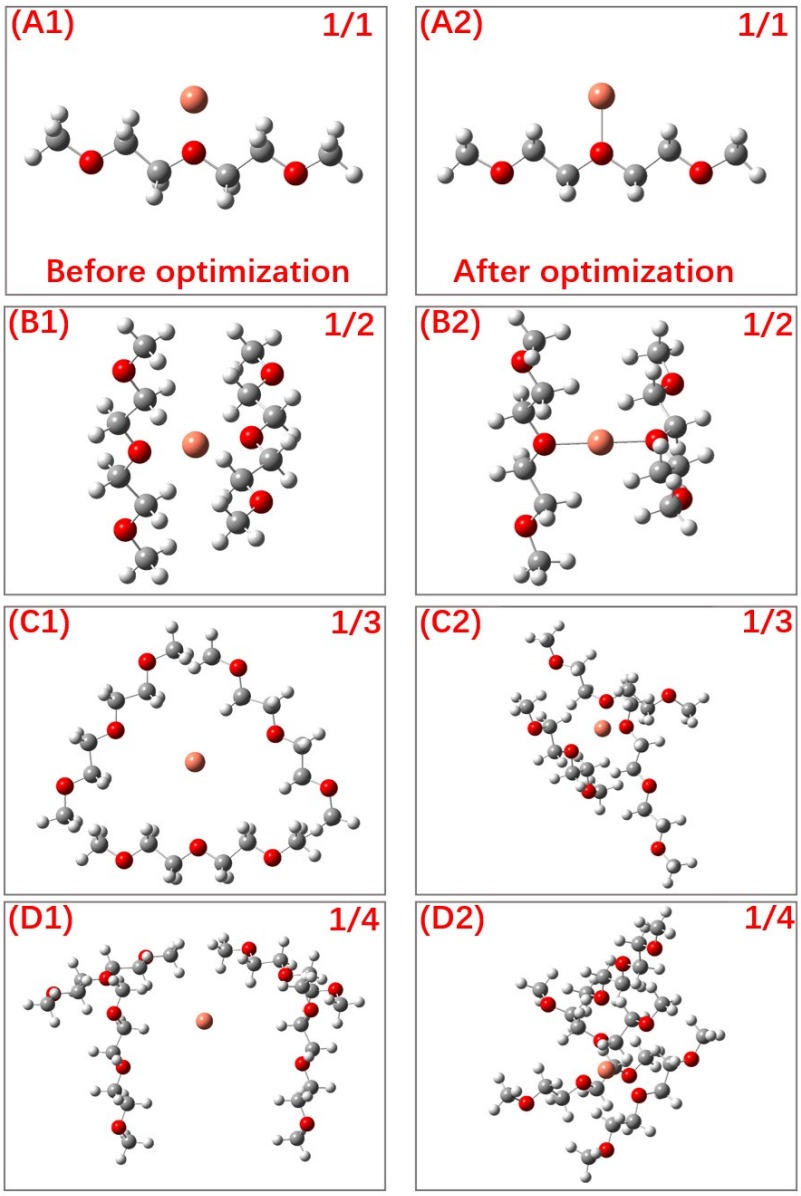

Fig.S11 The models of coordination with different contents before optimization and after optimization about Cu/DEGDME 1/1 (A1, A2), 1/2 (B1, B2), 1/3 (C1, C2) and 1/4 (D1, D2)

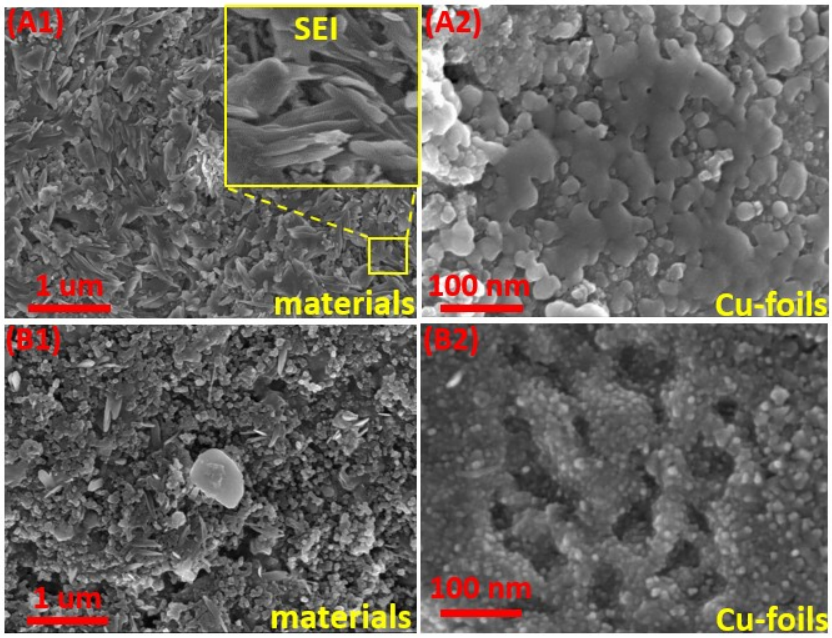

Fig.S12 SEM images of active materials, and relative Cu foils after 2000 cycles for FP (A1-A2), FPS-1 (B1-B2)

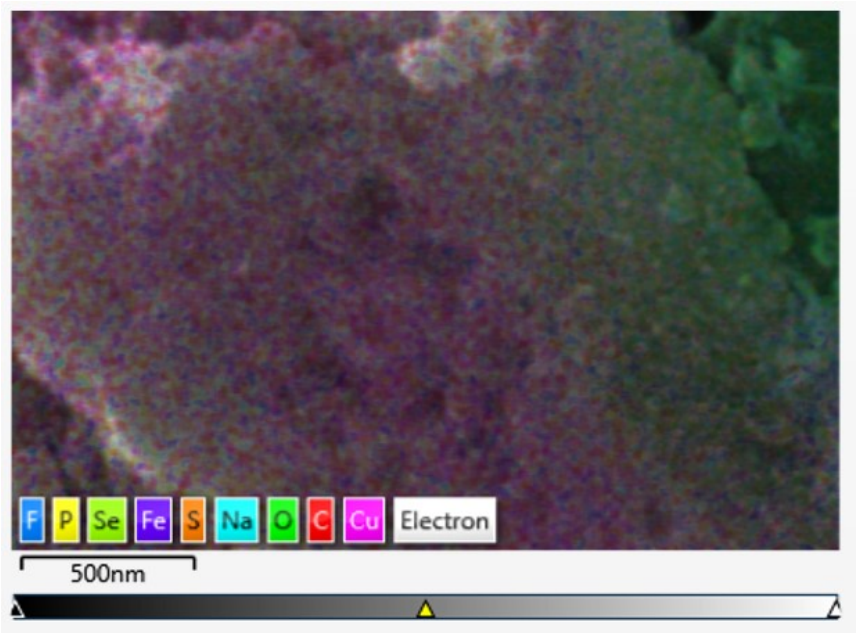

Fig.S13 Mapping images of FPS-2 after 2000 cycles

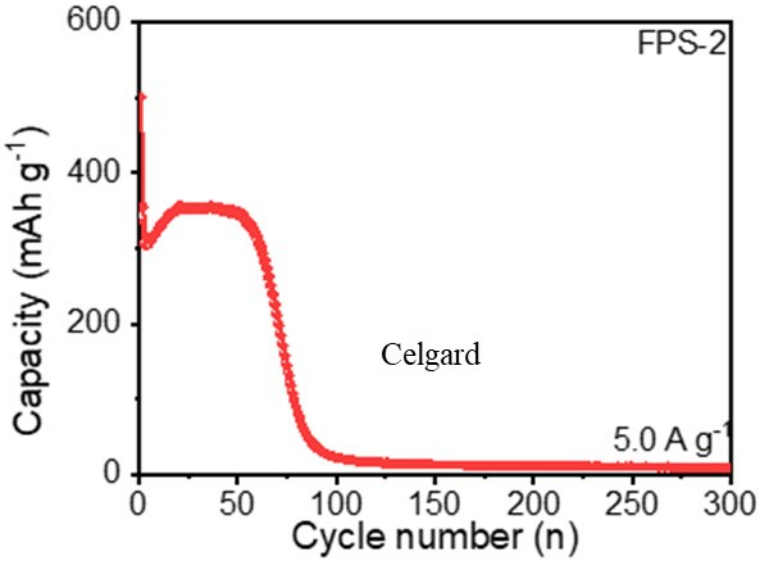

Fig.S14 Used Celgard as separations, the cycling stability of FPS-2 at 5.0 A g^{-1}

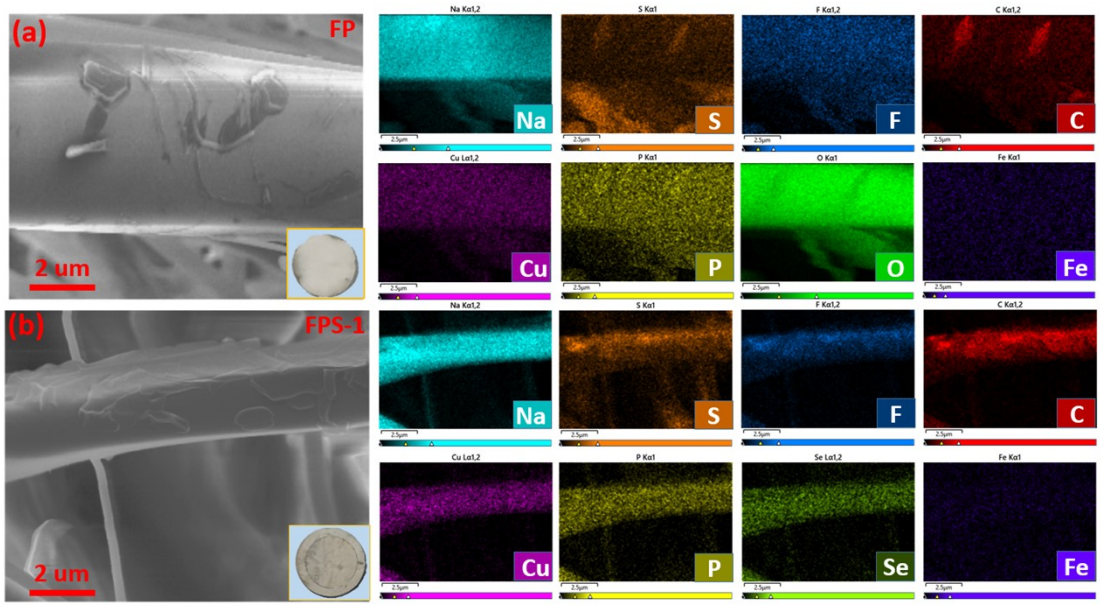

Fig.S15 SEM and Mapping images of separation (glass fiber) after 2000 cycles about FP (a), FPS-1 (b), the optical images in the inset of separations

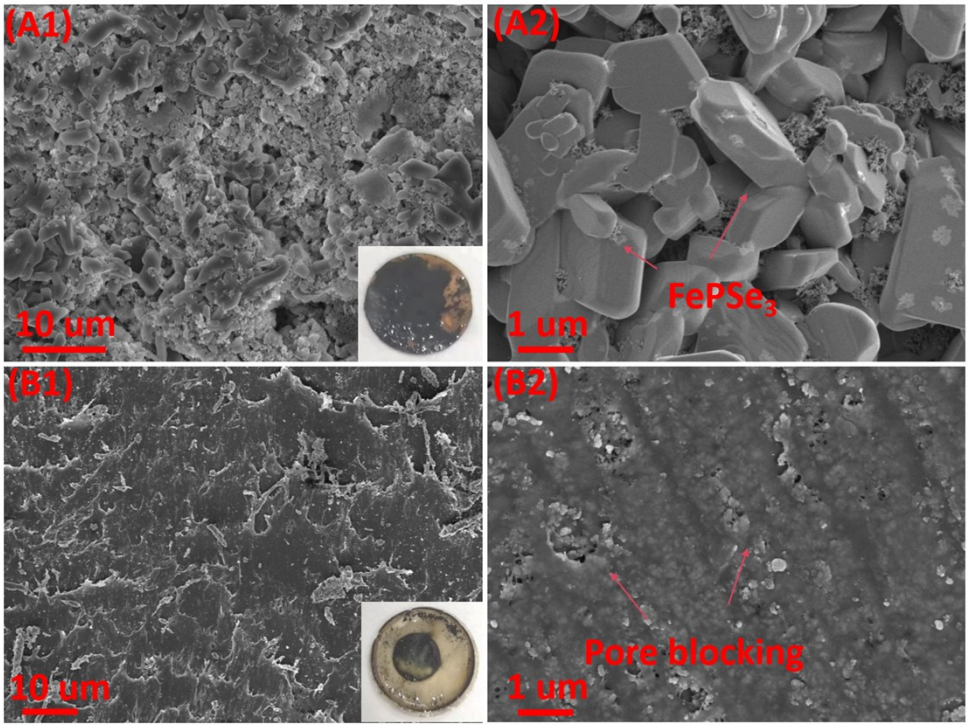

Fig.S16 Used Celgard as separations after 300 cycles: SEM images of Cu-foils (A1), active materials (A2), separations-Celgard (B1, B2), the corresponding optical images in the inset of separations